RSC Pharmaceutics

ROYAL SOCIETY OF CHEMISTRY

COMMUNICATION

View Article Online
View Journal | View Issue



Check for updates

Cite this: *RSC Pharm.*, 2024, **1**, 218

Received 1st December 2023,
Accepted 8th April 2024

DOI: 10.1039/d3pm00057e

rsc.li/RSCPharma

# Synthetic mucus barrier arrays as a nanoparticle formulation screening platform†

Harry Zou,‡ Allison Boboltz, ‡ Yahya Cheema, Daniel Song, Devorah Cahn and Gregg A. Duncan *

**A mucus gel layer lines the luminal surface of tissues throughout the body to protect them from infectious agents and particulates. As a result, nanoparticle drug delivery systems delivered to these sites may become trapped in mucus and subsequently cleared before they can reach target cells. As such, optimizing the properties of nanoparticle delivery vehicles, such as their surface chemistry and size, is essential to improving their penetration through the mucus barrier. In previous work, we developed a mucin-based hydrogel that has viscoelastic properties like that of native mucus which can be further tailored to mimic specific mucosal tissues and disease states. Using this biomimetic hydrogel system, a 3D-printed array containing synthetic mucus barriers was created that is compatible with a 96-well plate enabling its use as a high-throughput screening platform for nanoparticle drug delivery applications. To validate this system, we evaluated several established design parameters to determine their impact on nanoparticle penetration through synthetic mucus barriers. Consistent with the literature, we found nanoparticles of smaller size and coated with a protective PEG layer more efficiently penetrated through synthetic mucus barriers. In addition, we evaluated a mucolytic (tris(2-carboxyethyl) phosphine, TCEP) for use as a permeation enhancer for mucosal drug delivery. In comparison to *N*-acetyl cysteine (NAC), we found TCEP significantly improved nanoparticle penetration through a disease-like synthetic mucus barrier. Overall, our results establish a new high-throughput screening approach using synthetic mucus barrier arrays to identify promising nanoparticle formulation strategies for drug delivery to mucosal tissues.**

## Introduction

Mucus is continuously produced to form a protective layer in mucosal tissues throughout our body to prevent irritation, infection, and injury.[1–3] To eliminate pathogenic and other hazardous materials, mucus physically blocks and/or chemically binds to micro- and nanoscale particles depending on their size and surface chemistry. It has been shown that these barrier functions of mucus can limit the bioavailability of nanoparticle (NP) formulations given orally or administered locally to the eye, nose, lung, and vaginal tract.[4–7] For example, previous work has demonstrated nanoparticles with hydrophobic properties are strongly adherent to the mucus gel and quickly eliminated from the respiratory and reproductive tract.[8,9] In contrast, NP formulated with a dense surface coating of polyethylene glycol (PEG) were found to efficiently penetrate the mucus barrier and widely distribute within mucosal tissues. Enhancements in mucus penetration by PEGylated NP can be largely attributed to their near-neutral charge and hydrophilic surfaces which avoid adhesive interactions with the net-negatively charged and hydrophobic regions of mucin glycoproteins.[10,11]

In addition to PEGylation, several alternative strategies have been explored to facilitate NP passage through the mucus barrier such as peptide and zwitterionic polymer coatings as well as the co-administration of NP with mucus-degrading agents (mucolytics).[12–16] Moreover, the optimal dimensions of NP formulations (*e.g.* effective diameter, shape) can also vary depending on the target tissue. For example, the characteristic pore size of the mucus barrier can vary from as low as 20 nm in the adherent mucus layer in the gastrointestinal (GI) tract to up to 500 nm in the cervicovaginal tract.[17,18] In comparison to traditionally spherical NP, prior work has also demonstrated enhanced penetration of rod-shaped NP through mucus in the GI tract.[19,20] It is also important to note mucus barrier properties can be significantly altered as a function of disease which may lead to improved or limited NP penetration to the underlying tissue.[21–23] This prior research highlights the numerous concepts and approaches that one may consider in the design of NP formulations for mucosal drug delivery.

To optimize nanoparticle formulations for mucosal delivery, several assays have been established to directly measure mucus penetration efficiency. Early work primarily used

*Fischell Department of Bioengineering, University of Maryland, College Park, MD 20742, USA. E-mail: gaduncan@umd.edu*

†Electronic supplementary information (ESI) available. See DOI: https://doi.org/10.1039/d3pm00057e

‡These authors contributed equally to this work.

diffusion chambers where mucus collected from animals or humans is placed between donor and acceptor compartments where the fraction of particles that reach the acceptor chamber is monitored over time.[24] Microscopy-based methods such as fluorescence recovery after photobleaching (FRAP) and particle tracking are now often used to directly measure nanoparticle diffusion within mucus.[25–28] However, the methods available to assess NP transport through the mucus barrier are generally low-throughput which limits the ability to directly compare a wide range of formulation strategies. Moreover, it is often difficult to acquire mucus samples from humans to perform these assessments. Given the wide range of design parameters, it would be desirable to assess many NP formulations in parallel to down-select potential mucosal delivery strategies for further evaluation. In addition, the high-throughput system should be able to capture the changes in mucus properties as a function of tissue type and disease state.

Towards this end, we report a new strategy to screen nanoparticle formulations for mucosal delivery applications. Specifically, we developed a synthetic mucus barrier array (SMBA) platform containing mucin-based hydrogels which can be tailored to mimic the viscoelastic properties of native mucus in health and disease.[29–31] To confirm the validity of the SMBA system, we performed studies using polystyrene (PS) NP with size and surface chemistries previously evaluated in the literature. Based on the use of NAC as a mucolytic agent to enhance the penetration of NP through hyper-concentrated mucus produced in cystic fibrosis lung disease,[16,32] we then evaluated a newly identified mucolytic agent TCEP to determine its effectiveness as an NP permeation enhancer. Our data establishes proof-of-concept SMBA can be used to screen candidate NP formulations prior to further *in vitro* and *in vivo* evaluation for oral, inhaled, and topical drug delivery applications.

## Materials and methods

### Synthetic mucus hydrogel formulation

The synthetic mucus (SM) hydrogel used within the arrays was previously developed to mimic the material properties of human mucus.[29] A solution of 4% w/v porcine gastric mucins (PGM; Sigma Aldrich; mucin from porcine stomach, type III, bound sialic acid 0.5–1.5%, partially purified powder) was stirred for 2 hours in a physiological buffer representative of the ionic concentrations found in mucus (154 mM NaCl, 3 mM $CaCl_2$, and 15 mM $NaH_2PO_4$ adjusted to pH 7.4). Four arm-PEG-thiol (PEG-4SH, 10 kDa; Laysan Bio) was used as a crosslinking agent to form disulfide bonds between the mucins. A 4% w/v solution of PEG-4SH was prepared separately using the same physiological buffer. The 4% w/v solution of PGM and 4% w/v solution of PEG-4SH were combined in an equal volume ratio. The resulting SM hydrogels consisted of 2% w/v PGM and 2% w/v PEG-4SH, and are referred to as 2% SM gels. In experiments that utilized a 4% SM gel to mimic disease-state mucus, 8% w/v PGM and 8% w/v PEG-4SH solutions were prepared in the same manner and combined in equal volume ratios.

### Synthetic mucus barrier array design and preparation

Synthetic mucus barrier arrays (SMBA) were designed using computer-aided design software (Fusion360) with 9 wells that fit into an underlying 96-well flat black plate (Costar). An engineering drawing of the SMBA part is included in the ESI (Fig. S1†) and the file used to 3D print the part can be found as an additional ESI.† The SMBA devices were 3D printed using an SLA Formlabs 2 printer with V4 white resin material. The SM hydrogels were manually cast so they achieved gelation within the wells of the array. In order to cast hydrogels into the SMBA, parafilm was stretched across the surface of the 96-well plate, then the bottom of the wells of the SMBA were pressed downward into the wells of the plate. This technique formed a tight seal of parafilm over the bottom of the SMBA wells. The hydrogel solution was added using a pipette to the bottom of each well of the SMBA in the 96-well plate to allow for gelation in an upright position with the parafilm kept taut. The standard volume of hydrogel solution added to each well of the array devices was 30 μl, unless otherwise indicated. Assuming the gel maintains a cylindrical geometry within the SMBA, the hydrogel layer would possess a thickness of ~2 mm. The 96-well plate containing the SMBA was incubated for 22 hours in a humidified chamber to prevent drying out of the hydrogels during gelation. The SMBA was then taken out of the 96-well plate with care taken to ensure that the gels were not disturbed while peeling them off the parafilm. The standard volume of 30 μl was found to be the minimum volume that could be used where the gels would remain intact in the SMBA for the duration of experiments (up to 2 hours). Use of volumes less than <30 μl lead to incomplete gel coverage and leakiness within the SMBA which precluded testing at shorter total mucus gel depths. In addition, we have empirically determined 2 hours is the longest time we can consider without concern of hydrogel degradation due to swelling. Based on theoretical calculations, we expect nanoparticle diffusion alone is insufficient to cross the SMBA on the order of hours and anticipate sedimentation-driven transport is necessary for nanoparticle permeation in this timeframe. As such, a 2-hour timepoint was selected as a standard timepoint of sufficient duration to enable sedimentation equilibrium to be reached.

### Nanoparticle preparation

NP were rendered muco-inert with a dense surface coating of polyethylene glycol (PEG). Carboxylate-modified fluorescent PSNP with diameters of 20 nm, 100 nm, and 500 nm (Life Technologies) were coated with PEG. To minimize autofluorescence, fluorescent PSNP were used that emit in the red to far-red region with excitation/emission of either 580 nm/605 nm for 100 nm and 500 nm PS NP or 625 nm/645 nm for 20 nm PS NP. Five kDa methoxy PEG-amine (Creative PEGworks) was attached to the surface of theNP by a carboxyl-amine linkage, as previously described,[28,29] The zeta potential of PEG-coated NP (PS-PEG NP) was measured using a Nanobrook Omni

Particle Analyzer (Brookhaven Instruments). Measured zeta potential for 20 nm, 100 nm, and 500 nm were 0.02 ± 4.12 mV, −2.65 ± 0.90 mV, and −8.50 ± 1.57 mV, respectively. Using a previously established protocol,[33] we have also determined this approach yields PEG coatings within the dense brush regime *via* PEG density measurements (Table S1†).

### Determining nanoparticle penetration efficiency using SMBA

SMBAs with solidified gels were placed into a fresh 96-well black plate (Costar) with 100 μl of PBS added to the wells of the plate. NP were diluted in PBS prior to addition to the SMBA. The standard volume of NP solution added to the SMBA wells, unless otherwise indicated, was 10 μl. In experiments in which the mucolytics TCEP or NAC are used, the mucolytic was added directly into the solution ofNP in PBS at a concentration of 10 mM. As shown in Fig. 1, the gels were submerged in the 96-well plate containing PBS. The gels were then incubated after the addition of the NP solution for 2 hours at room temperature before the SMBAs and gels were removed from the 96-well plate. Positive control wells were also included in the 96-well plate, where the same NP solution added to the SMBA wells was added directly to the PBS in the 96-well plate. The positive control wells were used as a reference to determine the fluorescence of the full amount ofNP added to each SMBA well, simulating 100% penetration of NP, to aid in calculating the percent penetration of the NP across the gels in the experimental wells of SMBAs. A standard curve of serial dilutions ofPS NP from the stock solution was made in the same 96-well plate to allow for conversion between fluorescence units and known NP concentration. Then, a fluorescence reading was taken to assess the concentrationof NP in the PBS within the 96-well plate. The percentage of NP to penetrate the gels in the experimental wells was calculated by converting the fluorescence units measured in each well to NP concentration based on the standard curve. Finally, the percent penetration of NP across the gels was found by dividing the concentration in the experimental wells by the averaged concentration of NP in the positive control wells.

## Results & discussion

### NP size and surface chemistry affect their penetration through SMBA

For initial validation of the SMBA screening system, several parameters known to impact NP penetration through the mucus barrier were assessed (Fig. 2A). As noted, NP charge and hydrophobicity must be optimized to avoid adhesive interactions with the mucus barrier.[5,11] To assess the effect that NP surface chemistry has on penetration, 20 nm and 100 nm NP were coated with poly-ethylene glycol (PEG) to neutralize their surface charge. Carboxylate-modified PS and PS-PEGNP were added topically to the 2% SM hydrogels within the SMBA system and the fraction of NP to cross the synthetic mucus barrier in 2 hours was measured (Fig. 2B). PEGylatedNP in both sizes (20 nm and 100 nm) displayed significantly higher percent penetration than their non-PEGylated counterparts in the SMBA system. We then evaluated the effect of NP size on particle penetration. Percent penetration of 20 nm, 100 nm, and 500 nm PS-PEGNP across the SMBA system was compared (Fig. 2C). The results seen were consistent with prior studies[8,17,28] as we observed a negative correlation between NP size and particle penetration across the synthetic mucus barrier. These experiments validate that the SMBA system can accurately predict how these conditions impact particle penetration, by demonstrating that changes in NP surface chemistry and size will affect particle penetration in a manner consistent with previous studies. In addition, in experimental conditions where no particle penetration was observed (*e.g.* 500 nm PS-PEG and 100 nm PS), there was very little variability

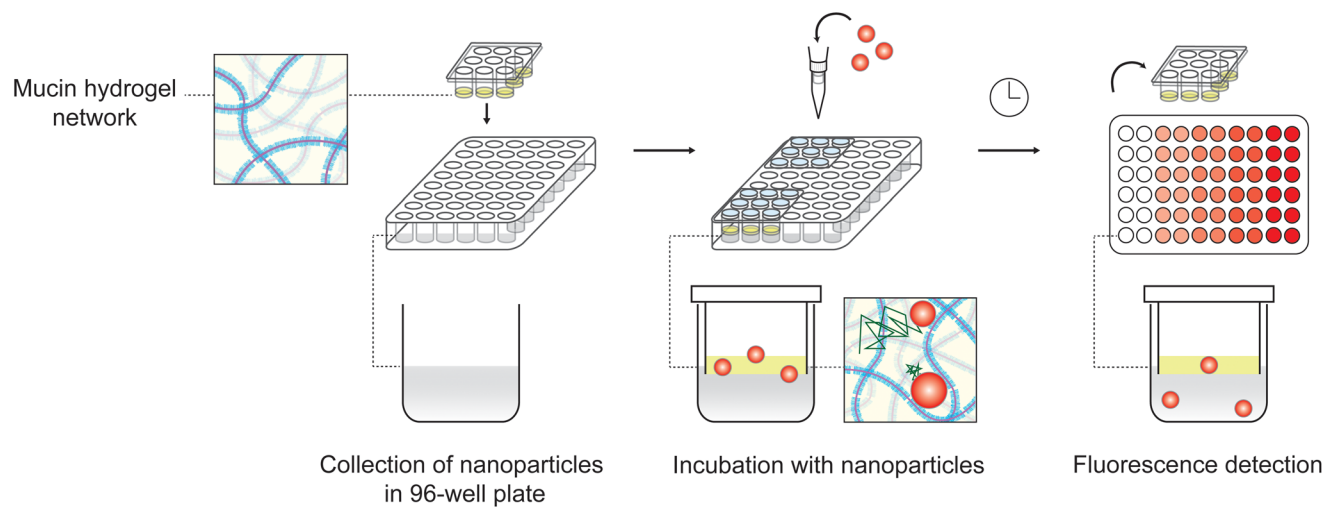


**Fig. 1** Schematic of SMBA experimental setup. SM hydrogels are cast in the wells of the SMBA device, then placed in a 96 well plate containing PBS. A solution of fluorescent NP is added to the apical surface of the gels.NP that penetrate the SM gel are detected *via* fluorescence.

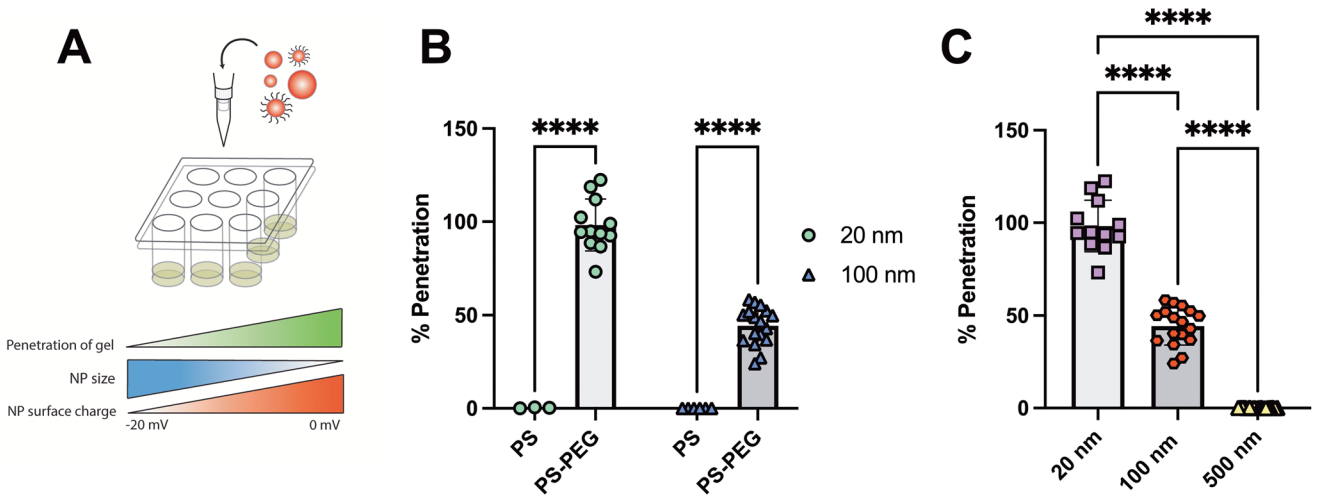


**Fig. 2** NP size and surface chemistry affect their penetration through SMBA. (A) Schematic of the effects of NP size and surface charge on SM gel penetration. (B) Comparison the percentage of PS NP (highly negative surface charge) *versus* PS-PEGNP (neutral surface charge) to penetrate 2% SM gels in the SMBA device, repeated with both 20 nm and 100 nmNP. (C) Penetration of PS-PEGNP across 2% SMgels in the SMBA device with various diameters (20 nm, 100 nm, 500 nm).

between wells which provides indirect evidence that hydrogel integrity is preserved across experiments.

### Impact of barrier thickness and solution volume on NP penetration through SMBA

To further assess NP penetration through SMBA under varying conditions, we next determined the effect of gel thickness and NP solution volume on NP penetration (Fig. 3A). To vary the gel thickness, 2% SM gels were cast in the SMBA device in two different volumes of either 30 µl, designated as a low gel volume, or 50 µl, designated as a high gel volume. Both 20 nm and 100 nm PS-PEG NP were then added topically to the SM hydrogels within the SMBA system and percent particle penetration was evaluated (Fig. 3B). A negative correlation was seen between the SM hydrogel volume and NP penetration of the gel as both 20 nm and 100 nm PS-PEG NP groups displayed significantly lower percent particle

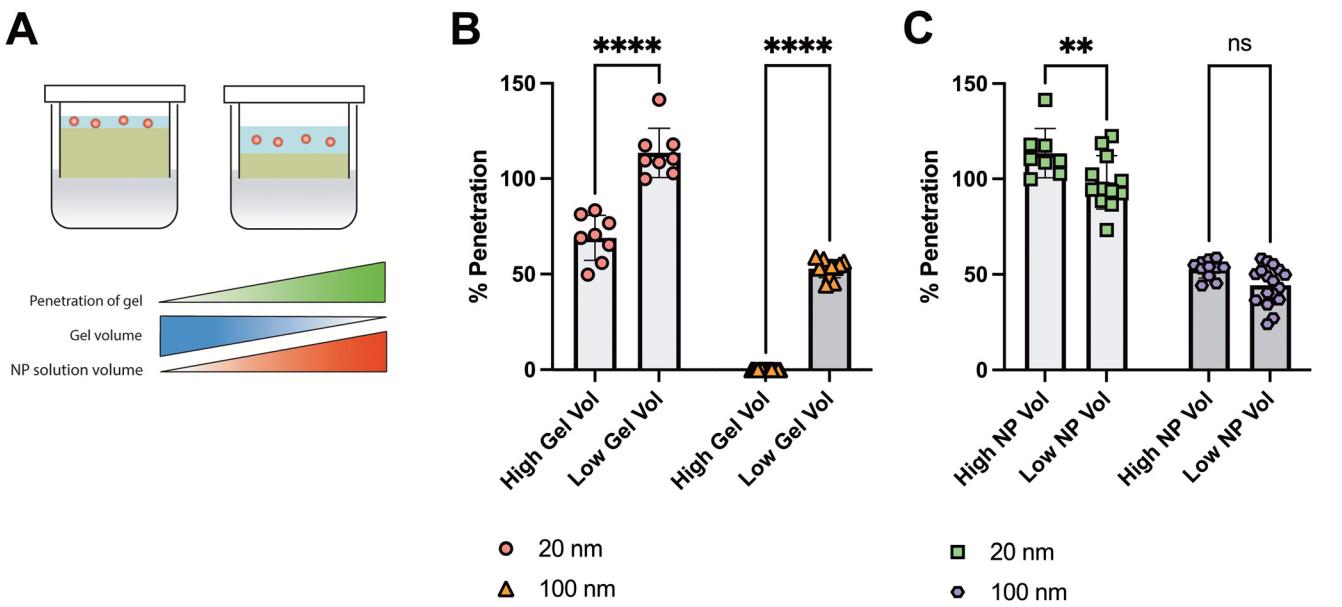


**Fig. 3** Impact of barrier thickness and solution volume on NP penetration through SMBA. (A) Schematic of the effects of varying either the SM gel volume or NP solution volume added to the SMBA device on diffusion across the SM gels. (B) 2% SM gels were cast in the SMBA device in two different volumes of either 30 l (low gel vol) or 50 l (high gel vol), then the percentage of both 20 nm and 100 nm PS-PEG NP to penetrate the gels was quantified. (C) Percent penetration across SM gels in the SMBA device of both 100 nm and 20 nm PS-PEGNP suspended in PBS solution applied in two different volumes of either 10 µl (low NP vol) or 20 µl (high NP vol). Statistical significance determined by two-way ANOVA with Šídák's multiple comparisons test (B and C). (ns = $p > 0.05$, **** = $p < 0.0001$, ** = $p < 0.01$).

penetration in the higher gel volume (50 μl) SM hydrogels within the SMBA system. This can likely be attributed to a larger effective distance that the NP must travel to penetrate a mucus barrier of greater thickness. However, an inherent limitation of SMBA that should be noted is the gel thicknesses evaluated (on the order of millimeters) are much larger than mucus layers found *in vivo*. As such, findings from the SMBA cannot be directly translated to more complex biological and animal models. Nonetheless, the SMBA system provides an initial screening tool to identify optimal NP formulations capable of penetrating the mucus barrier over time scales relevant to drug delivery applications.

We then analyzed the effect of NP solution volume administered topically to the SM hydrogels within the SMBA system (Fig. 3C). We examined percent particle penetration across 2% SM gels within the SMBA system of both 20 nm and 100 nm PS-PEG NP suspended in PBS solution in dosage volumes of either 10 μl, a relatively low NP volume, or 20 μl, a relatively high NP volume. A positive correlation was seen between the size of the NP solution administered and the percent of particle penetration seen in the 20 nm NP group, as a high NP solution volume (20 μl) had a statistically significantly higher percentage of NP penetration when compared to the low NP solution volume (10 μl). It is important to note that although this trend was seen, both groups had a high percent particle penetration (~90–100%). Although a similar trend was observed within the 100 nm NP group, no statistically significant difference was observed between the high NP solution volume and low NP solution volume groups. Thus, changing the volume of NP administered should not significantly impact the ability of the SMBA to detect differences in NP penetration between different conditions.

### Evaluating mucolytics as permeation enhancers for inhaled NP delivery using SMBA

In many chronic lung diseases such as asthma and cystic fibrosis, hyper-concentrated mucus is produced which may further limit the penetration of NP delivery systems under evaluation for inhaled drug and gene delivery.[25,34–36] To model disease-like conditions, we increased the total gel solids concentration and then assessed NP penetration using SMBA (Fig. 4A). We

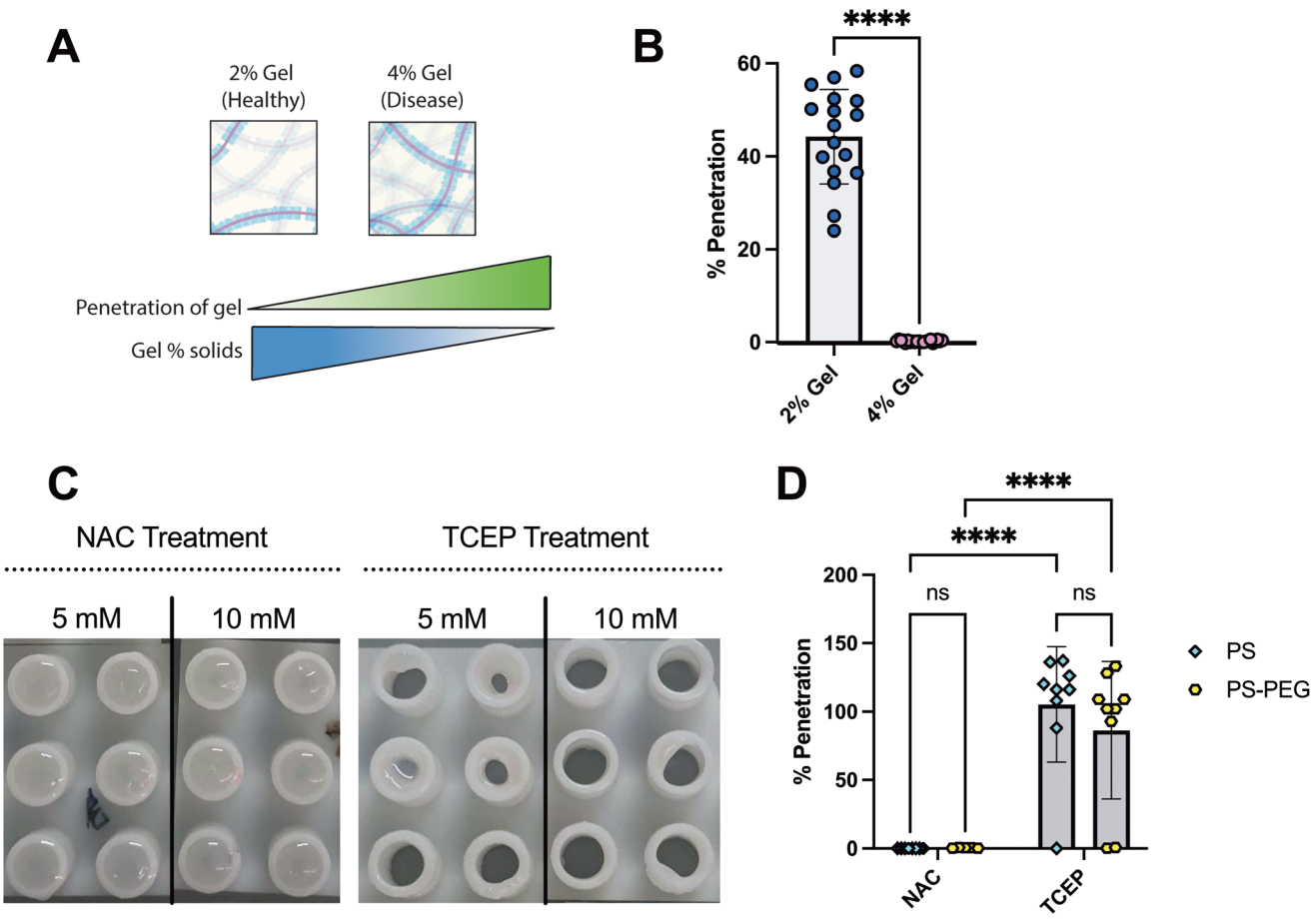


**Fig. 4** Evaluating mucolytics as permeation enhancers for inhaled NP delivery using SMBA. (A) Schematic of the effects of gel solids on NP penetration of the SM gel. (B) Comparison of 100 nm PS-PEG NP penetration through either 2% SM or 4% SM gels in the SMBA devices representing healthy and disease state mucus, respectively. (C) Images of the bottom of the SMBA devices containing 4% SM gels after treatment with the mucolytics NAC or TCEP at both 5 mM and 10 mM concentrations. (D) Percent penetration of 100 nm PS or PS-PEG NP when applied to 4% SM gels in the SMBA device in combination with either 10 mM TCEP or NAC. Statistical significance determined by unpaired *t*-test (B) and two-way ANOVA with Fisher's Least Significant Difference *post hoc* test (D). (ns = $p > 0.05$, **** = $p < 0.0001$).

prepared 2% SM gels to represent airway mucus in health and 4% synthetic mucus gels to represent mucus in individuals with obstructive lung disease.[23,37,38] We observed that percent particle penetration of the 100 nm PS-PEG NP was significantly reduced in the SMBA containing 4% SM gels when compared to the SMBA with healthy state 2% SM gels (Fig. 4B). These results highlight the potential utility of SMBA to examine the impact of alterations to the mucus barrier in disease. Given the significantly limited penetration of 100 nm NP under disease conditions, we then tested the impact of reducing agents, often used as mucolytic therapies, to enhance NP permeation through SMBA. We compared two mucolytic agents used as therapeutics to improve clearance of airway mucus: *N*-acetylcysteine (NAC), and tris(2-carboxyethyl) phosphine (TCEP).[35,39,40] Both NAC and TCEP act as mucolytics by reducing mucin–mucin disulfide bonds which directly degrades the mucus gel and reduces its viscoelasticity. NAC has been previously used in conjunction with PEGylated NP where it has been shown to enhance NP penetration through the airway mucus barrier.[16,32] We hypothesized TCEP would significantly enhance NP penetration in comparison to NAC as it has been shown to possess a much higher activity at reducing mucin biopolymers[39,41] and in more recent work, TCEP has shown promise as a permeation enhancer for inhaled nanoparticle drug delivery.[42] To further test this, we formed 4% SM gels (disease state) within the SMBA and treated them with either NAC or TCEP. We visually observed a significant degradation of the synthetic mucus gel when treated with TCEP (Fig. 4C). We then examined the percent of particle penetration of 100 nm PS and PS-PEGNP when applied to 4% SM gels in the SMBA system in combination with either 10 mM TCEP or 10 mM NAC (Fig. 4D). We observed that both PS and PS-PEGNP can achieve significantly greater (~90–100%) penetration in SM hydrogels treated with TCEP when compared to SM hydrogels treated with NAC . The results of these studies suggest TCEP may be a better alternative to NAC given the observed improvements in NP penetration through the mucus barrier. Studies can also be conducted in the future to further optimize the concentration of TCEP required to enhance NP penetration through the mucus barrier.

## Conclusions

We demonstrated that the SMBA system can be used to predict the fate of nanomedicine in the mucus barrier. By examining the effects of NP surface chemistry and size as well as mucus barrier concentration and thickness, we were able to demonstrate the utility of the SMBA to evaluate nanoparticle-based therapeutics targeted toward mucosal environments. Our head-to-head comparison of NAC and TCEP as NP permeation enhancers highlighted how SMBA could be helpful in optimizing formulation strategies by considering disease-associated changes to the mucus barrier. This proof-of-concept study will be expanded in future research to other clinically relevant drug and gene delivery systems (*e.g.* biodegradable polymeric NP, lipid NP, extracellular vesicles, viral vectors)[43–47] to optimize their properties for mucus penetration and improved therapeutic effectiveness. Ultimately, this work provides a simple but powerful method to assess NP design strategies for therapeutic applications targeting mucosal tissues.

We hope these studies also can serve as a guide to researchers in the field who are interested in screening NP formulations for mucosal drug delivery under development within their labs. The SMBA design is freely available to anyone interested in making use of this model. We provide here recommendations for those who seek to integrate SMBA screening as a tool in their research:

- *Muco-adhesive nanoparticles as an internal control*: To ensure each well used in your analysis retains its integrity for the duration of your experiment, an internal control particle, sized-match nanoparticles that are known to be adhesive to mucus (*e.g.* PS-NP) can be used to verify the well has not degraded during testing. Measured penetration efficiencies greater than 1% for a muco-adhesive control particle would be indicative of a well within the SMBA that is likely to have been compromised.
- *Gel concentration and volume*: We found gels composed of 2% w/v mucin and PEG-4SH reliably distinguished mucus-penetrating and muco-adhesive nanoparticle systems and as such, this concentration serves as a good starting point for screening. If targeting disease conditions where mucus hyperconcentration is expected (*e.g.* cystic fibrosis), higher concentrations can be considered. As noted in the methods, a 30 μl gel volume was the minimum necessary to ensure our gels retained their integrity for duration of experiments.
- *Time point*: A set timepoint of 2 hours was used for all studies conducted which we believe is ideal for assessment of nanoparticles in the range of 100 nm or less. However, it is likely nanoparticles of smaller sizes, 20 nm or less, that shorter timepoints could be used for assessment of penetration efficiency.
- *Vehicle solution volume*: The volume of the vehicle solution containing NP of interest should not exceed that of the gel volume within the SMBA to reduce potential risks of gel dilution and subsequent degradation.

## Conflicts of interest

The authors declare no conflict of interest.

## Acknowledgements

This work was supported by the Burroughs Wellcome Fund Career Award at the Scientific Interface (to G. A. D.), Cystic Fibrosis Foundation (BOBOLT23H0 to A. B.), the National Science Foundation (2047794, 2129624 to G. A. D.), the UMD-NCI Partnership for Integrative Cancer Research Traineeship (to D. C.) and the National Institutes of Health (R01 HL160540, U19 AI162130 to G. A. D.).

## References

1 J. Witten, T. Samad and K. Ribbeck, Selective Permeability of Mucus Barriers, *Curr. Opin. Biotechnol.*, 2018, **52**, 124–133, DOI: 10.1016/j.copbio.2018.03.010.

2 R. A. Cone, Barrier Properties of Mucus, *Adv. Drug Delivery Rev.*, 2009, **61**(2), 75–85, DOI: 10.1016/j.addr.2008.09.008.

3 D. J. Thornton and J. K. Sheehan, From Mucins to Mucus: Toward a More Coherent Understanding of This Essential Barrier, *Proc. Am. Thorac. Soc.*, 2004, **1**(1), 54–61, DOI: 10.1513/pats.2306016.

4 L. M. Ensign, R. Cone and J. Hanes, Oral Drug Delivery with Polymeric Nanoparticles: The Gastrointestinal Mucus Barriers, *Adv. Drug Delivery Rev.*, 2012, **64**(6), 557–570, DOI: 10.1016/j.addr.2011.12.009.

5 D. Song, D. Cahn and G. A. Duncan, Mucin Biopolymers and Their Barrier Function at Airway Surfaces, *Langmuir*, 2020, **36**(43), 12773–12783, DOI: 10.1021/acs.langmuir.0c02410.

6 G. Lacroix, V. Gouyer, F. Gottrand and J.-L. Desseyn, The Cervicovaginal Mucus Barrier, *Int. J. Mol. Sci.*, 2020, **21**(21), 8266, DOI: 10.3390/ijms21218266.

7 M. Ruponen and A. Urtti, Undefined Role of Mucus as a Barrier in Ocular Drug Delivery, *Eur. J. Pharm. Biopharm.*, 2015, **96**, 442–446, DOI: 10.1016/j.ejpb.2015.02.032.

8 C. S. Schneider, Q. Xu, N. J. Boylan, J. Chisholm, B. C. Tang, B. S. Schuster, A. Henning, L. M. Ensign, E. Lee, P. Adstamongkonkul, B. W. Simons, S.-Y. S. Wang, X. Gong, T. Yu, M. P. Boyle, J. S. Suk and J. Hanes, Nanoparticles That Do Not Adhere to Mucus Provide Uniform and Long-Lasting Drug Delivery to Airways Following Inhalation, *Sci. Adv.*, 2017, **3**(4), e1601556, DOI: 10.1126/sciadv.1601556.

9 L. M. Ensign, B. C. Tang, Y.-Y. Wang, A. T. Terence, T. Hoen, R. Cone and J. Hanes, Mucus-Penetrating Nanoparticles for Vaginal Drug Delivery Protect against Herpes Simplex Virus, *Sci. Transl. Med.*, 2012, **4**(138), 138ra79–138ra79, DOI: 10.1126/scitranslmed.3003453.

10 Q. Xu, L. M. Ensign, N. J. Boylan, A. Schön, X. Gong, J.-C. Yang, N. W. Lamb, S. Cai, T. Yu, E. Freire and J. Hanes, Impact of Surface Polyethylene Glycol (PEG) Density on Biodegradable Nanoparticle Transport in Mucus Ex Vivo and Distribution in Vivo, *ACS Nano*, 2015, **9**(9), 9217–9227, DOI: 10.1021/acsnano.5b03876.

11 L. M. Ensign, C. Schneider, J. S. Suk, R. Cone and J. Hanes, Mucus Penetrating Nanoparticles: Biophysical Tool and Method of Drug and Gene Delivery, *Adv. Mater.*, 2012, **24**(28), 3887–3894, DOI: 10.1002/adma.201201800.

12 J. Leal, X. Peng, X. Liu, D. Arasappan, D. C. Wylie, S. H. Schwartz, J. J. Fullmer, B. C. McWilliams, H. D. C. Smyth and D. Ghosh, Peptides as Surface Coatings of Nanoparticles That Penetrate Human Cystic Fibrosis Sputum and Uniformly Distribute in Vivo Following Pulmonary Delivery, *J. Controlled Release*, 2020, **322**, 457–469, DOI: 10.1016/j.jconrel.2020.03.032.

13 V. V. Khutoryanskiy, Beyond PEGylation: Alternative Surface-Modification of Nanoparticles with Mucus-Inert Biomaterials, *Adv. Drug Delivery Rev.*, 2018, **124**, 140–149, DOI: 10.1016/j.addr.2017.07.015.

14 Y. Ma, Y. Guo, S. Liu, Y. Hu, C. Yang, G. Cheng, C. Xue, Y. Y. Zuo and B. Sun, pH-Mediated Mucus Penetration of Zwitterionic Polydopamine-Modified Silica Nanoparticles, *Nano Lett.*, 2023, **23**(16), 7552–7560, DOI: 10.1021/acs.nanolett.3c02128.

15 T. Pho and J. A. Champion, Surface Engineering of Protein Nanoparticles Modulates Transport, Adsorption, and Uptake in Mucus, *ACS Appl. Mater. Interfaces*, 2022, **14**(46), 51697–51710, DOI: 10.1021/acsami.2c14670.

16 J. S. Suk, S. K. Lai, N. J. Boylan, M. R. Dawson, M. P. Boyle and J. Hanes, Rapid Transport of Muco-Inert Nanoparticles in Cystic Fibrosis Sputum Treated with *N*-Acetyl Cysteine, *Nanomedicine*, 2011, **6**(2), 365–375, DOI: 10.2217/nnm.10.123.

17 S. K. Lai, Y.-Y. Wang, K. Hida, R. Cone and J. Hanes, Nanoparticles Reveal That Human Cervicovaginal Mucus Is Riddled with Pores Larger than Viruses, *Proc. Natl. Acad. Sci. U. S. A.*, 2010, **107**(2), 598–603, DOI: 10.1073/pnas.0911748107.

18 A. N. Round, N. M. Rigby, A. Garcia de la Torre, A. Macierzanka, E. N. C. Mills and A. R. Mackie, Lamellar Structures of MUC2-Rich Mucin: A Potential Role in Governing the Barrier and Lubricating Functions of Intestinal Mucus, *Biomacromolecules*, 2012, **13**(10), 3253–3261, DOI: 10.1021/bm301024x.

19 C. Bao, B. Liu, B. Li, J. Chai, L. Zhang, L. Jiao, D. Li, Z. Yu, F. Ren, X. Shi and Y. Li, Enhanced Transport of Shape and Rigidity-Tuned α-Lactalbumin Nanotubes across Intestinal Mucus and Cellular Barriers, *Nano Lett.*, 2020, **20**(2), 1352–1361, DOI: 10.1021/acs.nanolett.9b04841.

20 M. Yu, J. Wang, Y. Yang, C. Zhu, Q. Su, S. Guo, J. Sun, Y. Gan, X. Shi and H. Gao, Rotation-Facilitated Rapid Transport of Nanorods in Mucosal Tissues, *Nano Lett.*, 2016, **16**(11), 7176–7182, DOI: 10.1021/acs.nanolett.6b03515.

21 M. E. V. Johansson, H. Sjövall and G. C. Hansson, The Gastrointestinal Mucus System in Health and Disease, *Nat. Rev. Gastroenterol. Hepatol.*, 2013, **10**(6), 352–361, DOI: 10.1038/nrgastro.2013.35.

22 T. Hoang, E. Toler, K. DeLong, N. A. Mafunda, S. M. Bloom, H. C. Zierden, T. R. Moench, J. S. Coleman, J. Hanes, D. S. Kwon, S. K. Lai, R. A. Cone and L. M. Ensign, The Cervicovaginal Mucus Barrier to HIV-1 Is Diminished in Bacterial Vaginosis, *PLoS Pathog.*, 2020, **16**(1), e1008236, DOI: 10.1371/journal.ppat.1008236.

23 G. A. Duncan, J. Jung, A. Joseph, A. L. Thaxton, N. E. West, M. P. Boyle, J. Hanes and J. S. Suk, Microstructural Alterations of Sputum in Cystic Fibrosis Lung Disease, *JCI Insight*, 2016, **1**(18), e88198, DOI: 10.1172/jci.insight.88198.

24 N. N. Sanders, S. C. De Smedt, E. Van Rompaey, P. Simoens, F. De Baets and J. Demeester, Cystic Fibrosis Sputum: A Barrier to the Transport of Nanospheres,

*Am. J. Respir. Crit. Care Med.*, 2000, **162**(5), 1905–1911, DOI: 10.1164/ajrccm.162.5.9909009.

25 G. A. Duncan, J. Jung, J. Hanes and J. S. Suk, The Mucus Barrier to Inhaled Gene Therapy, *Mol. Ther.*, 2016, **24**(12), 2043–2053, DOI: 10.1038/mt.2016.182.

26 B. S. Schuster, D. B. Allan, J. C. Kays, J. Hanes and R. L. Leheny, Photoactivatable Fluorescent Probes Reveal Heterogeneous Nanoparticle Permeation through Biological Gels at Multiple Scales, *J. Controlled Release*, 2017, **260**, 124–133, DOI: 10.1016/j.jconrel.2017.05.035.

27 H. P. Patil, D. Freches, L. Karmani, G. A. Duncan, B. Ucakar, J. S. Suk, J. Hanes, B. Gallez and R. Vanbever, Fate of PEGylated Antibody Fragments Following Delivery to the Lungs: Influence of Delivery Site, PEG Size and Lung Inflammation, *J. Controlled Release*, 2018, **272**, 62–71, DOI: 10.1016/j.jconrel.2017.12.009.

28 B. S. Schuster, J. S. Suk, G. F. Woodworth and J. Hanes, Nanoparticle Diffusion in Respiratory Mucus from Humans without Lung Disease, *Biomaterials*, 2013, **34**(13), 3439–3446, DOI: 10.1016/j.biomaterials.2013.01.064.

29 K. Joyner, D. Song, R. F. Hawkins, R. D. Silcott and G. A. Duncan, A Rational Approach to Form Disulfide Linked Mucin Hydrogels, *Soft Matter*, 2019, **15**(47), 9632–9639, DOI: 10.1039/c9sm01715a.

30 D. Song, E. Iverson, L. Kaler, S. Bader, M. A. Scull and G. A. Duncan, Modeling Airway Dysfunction in Asthma Using Synthetic Mucus Biomaterials, *ACS Biomater. Sci. Eng.*, 2021, **7**(6), 2723–2733, DOI: 10.1021/acsbiomaterials.0c01728.

31 A. Boboltz, S. Yang and G. A. Duncan, Engineering *in Vitro* Models of Cystic Fibrosis Lung Disease Using Neutrophil Extracellular Trap Inspired Biomaterials, *J. Mater. Chem. B*, 2023, **11**(39), 9419–9430, DOI: 10.1039/D3TB01489D.

32 J. S. Suk, N. J. Boylan, K. Trehan, B. C. Tang, C. S. Schneider, J.-M. G. Lin, M. P. Boyle, P. L. Zeitlin, S. K. Lai, M. J. Cooper and J. Hanes, N-Acetylcysteine Enhances Cystic Fibrosis Sputum Penetration and, Airway Gene Transfer by Highly Compacted DNA Nanoparticles, *Mol. Ther.*, 2011, **19**(11), 1981–1989, DOI: 10.1038/mt.2011.160.

33 D. Cahn and G. A. Duncan, High-Density Branched PEGylation for Nanoparticle Drug Delivery, *Cell. Mol. Bioeng.*, 2022, **15**(5), 355–366, DOI: 10.1007/s12195-022-00727-x.

34 B. S. Schuster, A. J. Kim, J. C. Kays, M. M. Kanzawa, W. B. Guggino, M. P. Boyle, S. M. Rowe, N. Muzyczka, J. S. Suk and J. Hanes, Overcoming the Cystic Fibrosis Sputum Barrier to Leading Adeno-Associated Virus Gene Therapy Vectors, *Mol. Ther.*, 2014, **22**(8), 1484–1493, DOI: 10.1038/mt.2014.89.

35 N. Kim, G. A. Duncan, J. Hanes and J. S. Suk, Barriers to Inhaled Gene Therapy of Obstructive Lung Diseases: A Review, *J. Controlled Release*, 2016, **240**, 465–488, DOI: 10.1016/j.jconrel.2016.05.031.

36 L. Kaler, K. Joyner and G. A. Duncan, Machine Learning-Informed Predictions of Nanoparticle Mobility and Fate in the Mucus Barrier, *APL Bioeng.*, 2022, **6**(2), 026103, DOI: 10.1063/5.0091025.

37 D. B. Hill, P. a. Vasquez, J. Mellnik, S. a. McKinley, A. Vose, F. Mu, A. G. Henderson, S. H. Donaldson, N. E. Alexis, R. C. Boucher and M. G. Forest, A Biophysical Basis for Mucus Solids Concentration as a Candidate Biomarker for Airways Disease, *PLoS One*, 2014, **9**(2), 1–11, DOI: 10.1371/journal.pone.0087681.

38 M. R. Markovetz, D. B. Subramani, W. J. Kissner, C. B. Morrison, I. C. Garbarine, A. Ghio, K. A. Ramsey, H. Arora, P. Kumar, D. B. Nix, T. Kumagai, T. M. Krunkosky, D. C. Krause, G. Radicioni, N. E. Alexis, M. Kesimer, M. Tiemeyer, R. C. Boucher, C. Ehre and D. B. Hill, Endotracheal Tube Mucus as a Source of Airway Mucus for Rheological Study, *Am. J. Physiol.: Lung Cell. Mol. Physiol.*, 2019, **317**(4), L498–L509, DOI: 10.1152/ajplung.00238.2019.

39 L. E. Morgan, A. M. Jaramillo, S. K. Shenoy, D. Raclawska, N. A. Emezienna, V. L. Richardson, N. Hara, A. Q. Harder, J. C. NeeDell, C. E. Hennessy, H. M. El-Batal, C. M. Magin, D. E. Grove Villalon, G. Duncan, J. S. Hanes, J. S. Suk, D. J. Thornton, F. Holguin, W. J. Janssen, W. R. Thelin and C. M. Evans, Disulfide Disruption Reverses Mucus Dysfunction in Allergic Airway Disease, *Nat. Commun.*, 2021, **12**(1), 249, DOI: 10.1038/s41467-020-20499-0.

40 R. C. Boucher, Muco-Obstructive Lung Diseases, *N. Engl. J. Med.*, 2019, **380**(20), 1941–1953, DOI: 10.1056/nejmra1813799.

41 M. I. Pino-Argumedo, A. J. Fischer, B. M. Hilkin, N. D. Gansemer, P. D. Allen, E. A. Hoffman, D. A. Stoltz, M. J. Welsh and M. H. Abou Alaiwa, Elastic, Mucus Strands Impair Mucociliary Clearance in Cystic Fibrosis Pigs, *Proc. Natl. Acad. Sci. U. S. A.*, 2022, **119**(13), e2121731119, DOI: 10.1073/pnas.2121731119.

42 M. Yang, M. Han, L. Tang, Y. Bi, X. Li, J. Jeong, Y. Wang and H. Jiang, Dual Barrier–Penetrating Inhaled Nanoparticles for Enhanced Idiopathic Pulmonary Fibrosis Therapy, *Adv. Funct. Mater.*, 2024, 2315128, DOI: 10.1002/adfm.202315128.

43 G. A. Duncan, N. Kim, Y. Colon-Cortes, J. Rodriguez, M. Mazur, S. E. Birket, S. M. Rowe, N. E. West, A. Livraghi-Butrico, R. C. Boucher, J. Hanes, G. Aslanidi and J. S. Suk, An Adeno-Associated Viral Vector Capable of Penetrating the Mucus Barrier to Inhaled Gene Therapy, *Mol. Ther.–Methods Clin. Dev.*, 2018, **9**, 296–304, DOI: 10.1016/j.omtm.2018.03.006.

44 P. Mastorakos, A. L. da Silva, J. Chisholm, E. Song, W. K. Choi, M. P. Boyle, M. M. Morales, J. Hanes and J. S. Suk, Highly Compacted Biodegradable DNA Nanoparticles Capable of Overcoming the Mucus Barrier for Inhaled Lung Gene Therapy, *Proc. Natl. Acad. Sci. U. S. A.*, 2015, **112**(28), 8720–8725, DOI: 10.1073/pnas.1502281112.

45 Z. Wang, K. D. Popowski, D. Zhu, B. L. de Juan Abad, X. Wang, M. Liu, H. Lutz, N. De Naeyer, C. T. DeMarco, T. N. Denny, P.-U. C. Dinh, Z. Li and K. Cheng, Exosomes

Decorated with a Recombinant SARS-CoV-2 Receptor-Binding Domain as an Inhalable COVID-19 Vaccine, *Nat. Biomed. Eng.*, 2022, **6**(7), 791–805, DOI: **10.1038/s41551-022-00902-5**.

46 J. Kim, A. Jozic, Y. Lin, Y. Eygeris, E. Bloom, X. Tan, C. Acosta, K. D. MacDonald, K. D. Welsher and G. Sahay, Engineering Lipid Nanoparticles for Enhanced Intracellular Delivery of mRNA through Inhalation, *ACS Nano*, 2022, **16**(9), 14792–14806, DOI: **10.1021/acsnano.2c05647**.

47 M. P. Lokugamage, D. Vanover, J. Beyersdorf, M. Z. C. Hatit, L. Rotolo, E. S. Echeverri, H. E. Peck, H. Ni, J.-K. Yoon, Y. Kim, P. J. Santangelo and J. E. Dahlman, Optimization of Lipid Nanoparticles for the Delivery of Nebulized Therapeutic mRNA to the Lungs, *Nat. Biomed. Eng.*, 2021, **5**(9), 1059–1068, DOI: **10.1038/s41551-021-00786-x**.